Mechanical and functional properties of two-phase $Ni_{53}Mn_{22}Co_6Ga_{19}$ high-temperature shape memory alloy with the addition of Dy

2013 Smart Mater. Struct. 22 035008

(http://iopscience.iop.org/0964-1726/22/3/035008)

IOP PUBLISHING SMART MATERIALS AND STRUCTURES
Smart Mater. Struct. **22** (2013) 035008 (7pp) doi:10.1088/0964-1726/22/3/035008

Mechanical and functional properties of two-phase $Ni_{53}Mn_{22}Co_6Ga_{19}$ high-temperature shape memory alloy with the addition of Dy

S Y Yang, C P Wang and X J Liu

Department of Materials Science and Engineering, College of Materials, Xiamen University, Xiamen, 361005, People's Republic of China

E-mail: yangshuiyuan@xmu.edu.cn and lxj@xmu.edu.cn

Received 22 July 2012, in final form 31 December 2012
Published 4 February 2013
Online at stacks.iop.org/SMS/22/035008

Abstract
The effects of Dy addition on microstructure, martensitic transformation, mechanical and shape memory properties of the two-phase $Ni_{53}Mn_{22}Co_6Ga_{19}$ high-temperature shape memory alloy were investigated. It is found that a small Dy addition results in the refinement of grain size, which can effectively improve the tensile ductility and strength of the two-phase $Ni_{53}Mn_{22}Co_6Ga_{19}$ alloy. However, a $Dy(Ni, Mn)_4Ga$ precipitate forms in the alloys with the Dy addition, and its amount increases with an increase in the Dy addition. This change causes the ductility of the alloys to decrease when the Dy addition is further increased to 0.3 at.%. The results further show that the changes in the martensitic transformation temperature of the studied alloys can be attributed to the combined effects of the tetragonality (c/a) and electron concentration (e/a) of martensite. Additionally, the shape memory effects of the alloys are closely related to the refinement of grain size and the alloy strength. In this study, the $(Ni_{53}Mn_{22}Co_6Ga_{19})_{99.8}Dy_{0.2}$ alloy exhibits a variety of good properties, including a high martensitic transformation starting temperature of 385.7 °C, a tensile ductility of 10.3% and a shape memory effect of 2.8%.

(Some figures may appear in colour only in the online journal)

1. Introduction

Several previous investigations have already reported that Ni–Mn–Ga alloys show great potential as high-temperature shape memory alloys (HTSMAs) due to a variety of excellent properties [1–5], such as high martensitic transformation temperatures, good thermal stability, and a shape memory effect (SME) of over 6% in single-crystalline $Ni_{54}Mn_{25}Ga_{21}$ alloy. However, the high brittleness of polycrystalline Ni–Mn–Ga alloys is the biggest obstacle for their further development. As a result, current research and development work is focusing on improving their ductility. Recently, it has been revealed that introducing a ductile γ phase with a fcc structure into the martensite matrix of Ni–Mn–Ga alloys by alloying with elements such as Fe, Cu and Co, is an effective method to improve their tensile ductility [6–11]. In these previous reports, these 'modified' two-phase NiMnGa-based alloys could be successfully hot-rolled to smooth plates, and their mechanical and shape memory properties were studied by tensile tests. However, with an increase in the volume fraction of the γ phase, the SMEs of the alloys were significantly impaired because γ phase did not participate in the reversible martensitic transformation [6–11].

Additionally, it has been reported that the mechanical properties of Ni–Mn–Ga alloys can be improved through the refinement of grain size by adding rare earth elements, such as Dy, Gd, Tb, Sm, Y and Nd [12–19]. However, their investigations mostly focus on the single martensite

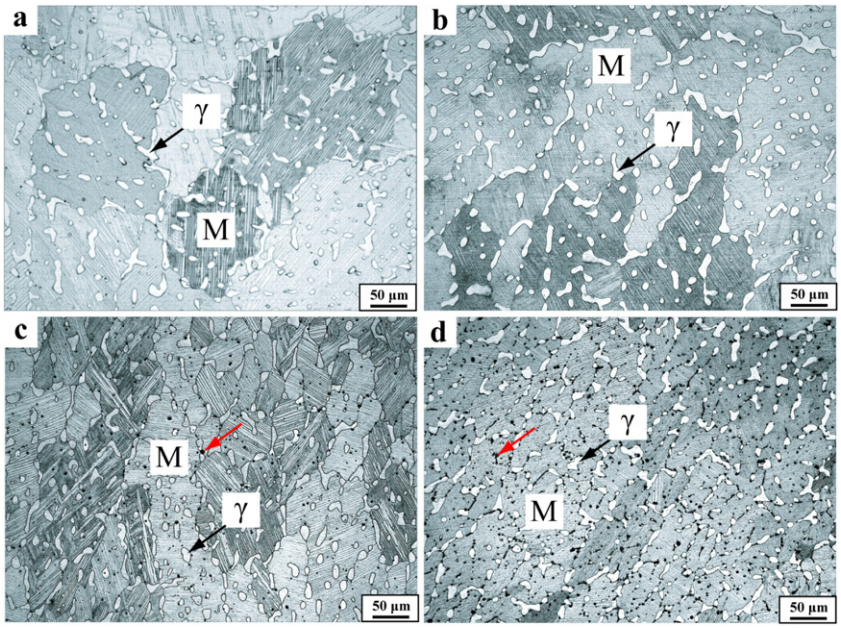

Figure 1. Optical micrographs of $(Ni_{53}Mn_{22}Co_6Ga_{19})_{100-x}Dy_x$ ($x = 0, 0.1, 0.2, 0.3$) alloys. (a) $x = 0$; (b) $x = 0.1$; (c) $x = 0.2$; (d) $x = 0.3$. *M* indicates martensite.

Ni–Mn–Ga alloys, and the ductility improvement of the alloys is limited. Until now, the effect of rare earth elements on two-phase NiMnGa-base alloys has not yet been investigated. The present study has been carried out to address this issue. In this study, a small amount of rare earth Dy is added into the two-phase $Ni_{53}Mn_{22}Co_6Ga_{19}$ master alloy in order to refine the grain size and thereby achieve a good combination of high martensitic transformation temperature, tensile ductility and shape memory effect in polycrystalline Ni–Mn–Ga alloys. This paper will present the results on the microstructures, martensitic transformation behaviors, and mechanical and shape memory properties of $(Ni_{53}Mn_{22}Co_6Ga_{19})_{100-x}Dy_x (x = 0, 0.1, 0.2, 0.3)$ alloys.

2. Experimental procedure

The purities of nickel, manganese, gallium, cobalt and dysprosium used are 99.9%, 99.7%, 99.99%, 99.9% and 99.5%, respectively. Four samples with nominal compositions of $(Ni_{53}Mn_{22}Co_6Ga_{19})_{100-x}Dy_x$ ($x = 0, 0.1, 0.2, 0.3$) (at.%), about 40 g each in weight, were arc-melted five times under the protection of an argon atmosphere to ensure homogeneity. The thus-prepared metal buttons were sealed under vacuum into quartz ampules and annealed at 900 °C for 3 days, followed by ice-water quenching. Some slices were cut from the as-quenched buttons by an electrical discharger for investigations of the phase structure, composition, microstructure and martensitic transformation behaviors. The remaining portions of the buttons were heated to 900 °C and hot-rolled to a final thickness of 1 mm at a reduction of about 0.5 mm per pass.

The microstructures were observed by optical microscopy (OM) and scanning electron microscopy (SEM) using the back-scattered electron (BSE) method. Samples for microscopic observation were mechanically polished and chemically etched in a solution of 99 ml methanol +2 ml nitric acid +5 g ferric chloride. Compositions of the phase constituents with an average value of five measurements and compositional mapping analysis were carried out by electron probe microanalysis (EPMA) (JEOL, JXA-8100). The crystallographic structure of the phases was identified at room temperature by x-ray diffraction using a Panalytical X'pert PRO with Cu K_α radiation. The martensitic transformation temperature was determined by differential scanning calorimetry (DSC) (Netzsch STA 404) at a rate of 10 °C min^{-1} for both the heating and cooling. The mechanical properties and SMEs were measured by tensile tests at ambient temperature using a Galdabini Sun 2500 machine at a crosshead speed of 0.2 mm min^{-1}. The tensile direction was parallel to the rolling direction. The gauge dimensions of the tensile specimens were about 2.5 mm wide, 1 mm thick and 9 mm long according to the relationship of $L_0 = 5.65 \times A^{1/2}$ [20], where A was the cross-sectional area and L_0 was the length of the gauge section. The lengths of the specimens were measured before loading (l_0), after unloading (l_1), and after heating to 600 °C for 5 min (l_2) by using a micrometer with an accuracy of 0.01 mm. The pre-strain during the tensile test was defined as $\varepsilon_{pre} = \Delta l/l_0$, where Δl was the displacement of the crosshead. The residual strain after unloading (ε_r), recovery strain (ε_{SME}) and recovery rate (R) were obtained as: $(l_1 - l_0)/l_0 \times 100\%$, $(l_1 - l_2)/l_0 \times 100\%$ and $(l_1 - l_2)/(l_1 - l_0) \times 100\%$, respectively.

3. Results and discussion

3.1. Microstructure

Figure 1 shows the optical micrographs of the $(Ni_{53}Mn_{22}Co_6Ga_{19})_{100-x}Dy_x$ ($x = 0, 0.1, 0.2, 0.3$) alloys. From figure 1, a

Table 1. Average compositions of the martensite and γ phase, and the e/a of martensite in $(Ni_{53}Mn_{22}Co_6Ga_{19})_{100-x}Dy_x$ ($x = 0$, 0.1, 0.2, 0.3) alloys.

	Martensite (at.%)				γ phase (at.%)				
Samples	Ni	Mn	Co	Ga	Ni	Mn	Co	Ga	e/a
$x = 0$	53.72	23.42	5.35	17.51	58.47	20.35	10.96	10.22	8.018
$x = 0.1$	51.26	23.73	6.12	18.88	56.52	22.58	11.11	9.79	7.904
$x = 0.2$	51.39	23.84	6.03	18.73	56.54	22.37	11.18	9.91	7.912
$x = 0.3$	51.45	23.88	6.06	18.61	56.49	21.38	11.24	10.89	7.920

two-phase structure can be clearly observed, consisting of a gray or black matrix and white small granular second phase. The matrix is the non-modulated martensite characterized by typical lamellar twin substructures denoted as *M*. The white small granular grains are confirmed to be a fcc γ phase, based on analyses of x-ray diffraction patterns, which will be detailed in a later section. These results have been already reported by the previous investigations [4, 7–11]. Interestingly, in the present study, the grain size of the alloys obviously decreases with increasing Dy content. These results are consistent with those obtained in the previous investigations when adding rare earth elements into the single martensite Ni–Mn–Ga alloys [13–16, 18, 19]. The compositions of the martensite and γ phase are determined by EPMA and listed in table 1. Also, it can be seen from figures 1(c) and (d) that small black spots are present, as shown by the red arrows. The BSE images of $x = 0.1$, 0.2 and 0.3 are shown in figure 2. In figure 2, these small particles appear as the white precipitate, not black spots as in figures 1(c) and (d). In fact, such precipitates are also present at $x = 0.1$, as seen in figure 2(a), but are not observed in figure 1(b) due to its minute quantity. The amounts of the precipitate gradually increase with an increase in the Dy addition.

The chemical compositions of the precipitate cannot be determined by EPMA due to its tiny grain size. Therefore, in this research, the compositional mapping analysis is carried out at $x = 0.3$, and the results are presented in figure 3. Figure 3(a) is the BSE image, figures 3(b)–(f) are the corresponding compositional maps of Dy, Mn, Co, Ga and Ni contents, respectively. From figure 3, it can be found that the Ni, Co and Ga contents of the precipitates are close to those of martensite in table 1, and the Mn content of the precipitates (about 14%) is obviously lower than the martensite and γ phase. Meanwhile, the Dy content of the precipitates (about 5%) is higher in the precipitates, whereas the Dy content in the martensite and γ phase is very close to zero. Therefore, the precipitates are referred to as the Dy-rich phase. Information available in the open literature [21–23] indicates that the solubility of Dy in the martensite phase in Ni–Mn–Ga alloys is very low, where the solubility of Dy means that a small amount of Dy dissolves in the martensite phase not leading to a change of its intrinsic crystal structure. Additionally, the atomic radius of Dy is about 1.5 times larger than those of the other elements and it can react with Ni, Mn, Co and Ga, possibly producing various intermetallic compounds [21–23]. Thus it is difficult for Dy to dissolve in the martensite and γ phase. These factors result in the precipitation and

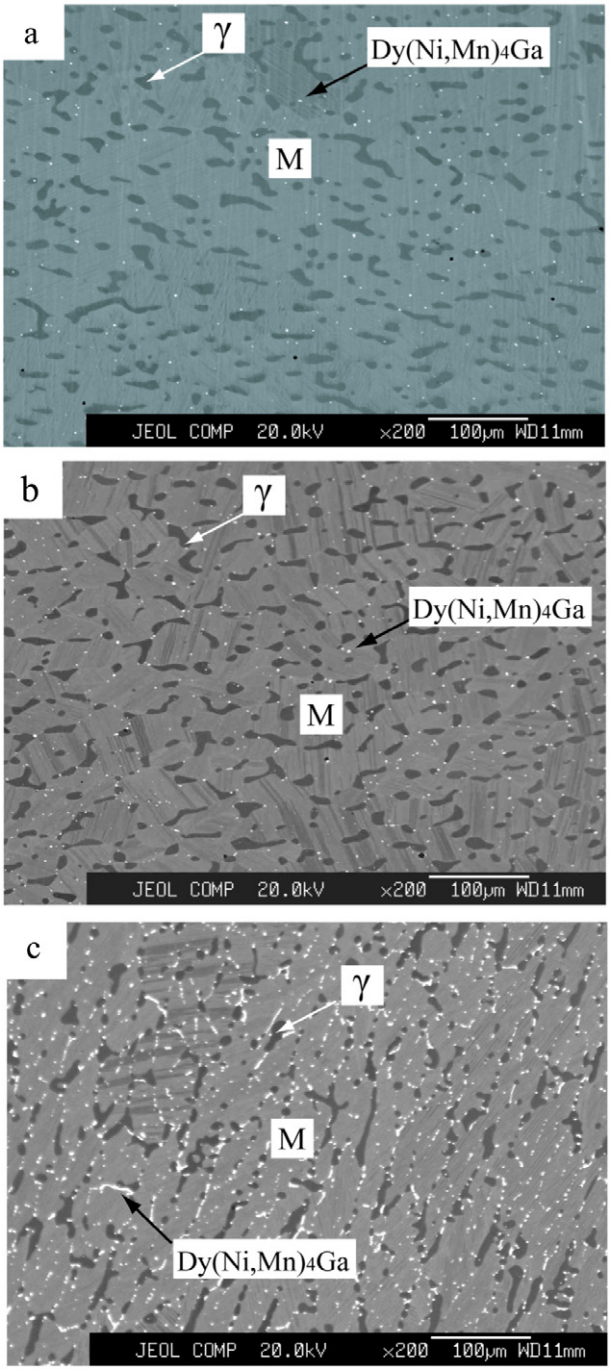

Figure 2. BSE images of $(Ni_{53}Mn_{22}Co_6Ga_{19})_{100-x}Dy_x$ ($x = 0.1$, 0.2, 0.3) alloys. (a) $x = 0.1$; (b) $x = 0.2$; (c) $x = 0.3$. *M* indicates martensite.

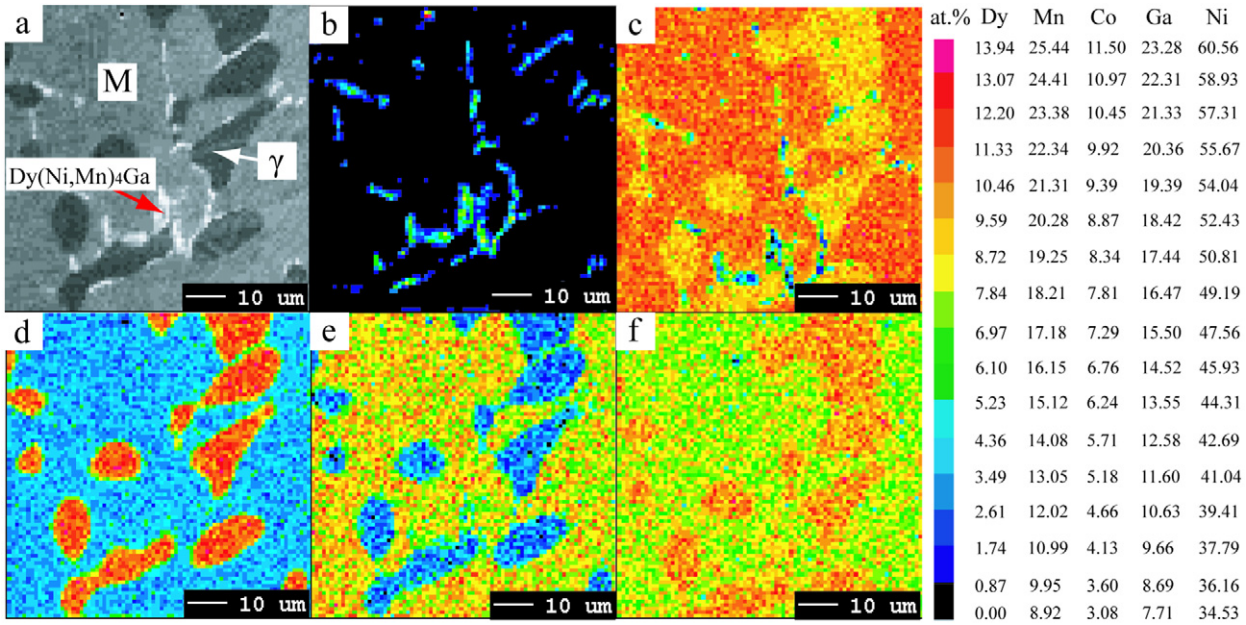

Figure 3. Compositional mapping analysis of $(Ni_{53}Mn_{22}Co_6Ga_{19})_{99.7}Dy_{0.3}$ alloy. (a) BSE image; (b) Dy; (c) Mn; (d) Co; (e) Ga; (f) Ni. *M* indicates martensite.

growth of the Dy-rich phase. Similar results can be found in previous investigations of $Ni_{50}Mn_{29}Ga_{21-x}Dy_x$ alloys [18, 19]. In those investigations, the Dy-rich phase was present when the Dy content of the alloy reached 0.1 at.%. Also, it was confirmed as the Dy(Ni, Mn)$_4$Ga phase with the $CaCu_5$ type hexagonal structure by XRD and transmission electron microscopy (TEM). Additionally, similar Gd(Ni, Mn)$_4$Ga and Y(Ni, Mn)$_4$Ga phases also existed in $Ni_{50}Mn_{29}Ga_{16}Gd_5$ and $Ni_{50}Mn_{29}Ga_{21-x}Y_x$ alloys [13–16]. Meanwhile, D.A. Joshi *et al* [24] have synthesized and studied a series of RNi_4Ga (R = rare earth, including Gd and Dy) compounds. Based on the above information, and comparing with the results of the compositional mapping analysis in figure 3, it can be confirmed that the Dy-rich phase in the present study is the Dy(Ni, Mn)$_4$Ga phase.

X-ray diffraction patterns of $(Ni_{53}Mn_{22}Co_6Ga_{19})_{100-x}Dy_x (x = 0, 0.1, 0.2, 0.3)$ alloys at room temperature are shown in figure 4. All the reflection patterns can be indexed by two phases containing the martensite and face-centered cubic (fcc) γ phase, similar to the previous investigations [8–11] and the results in figure 1. The lattice parameters of the martensite are calculated and summarized in table 2. It can be found that the tetragonality (c/a) and unit-cell volume of martensite abruptly increase when adding 0.1 at.% of Dy. The reason is that the small amount Dy with a larger atomic radius dissolves in martensite, which leads to a distortion of martensite crystal lattice. Interestingly, the tetragonality (c/a) variation mainly depends on the increased c value with 0.1 at.% of Dy addition, while a is almost constant. The reasons for such a phenomenon are still unclear. However, some factors might be considered to be related to this situation. For example, the dissolved Dy atom in martensite tends to occupy the octahedral or/and tetragonal interstice site of martensite. More investigations will be needed on this point. But on further

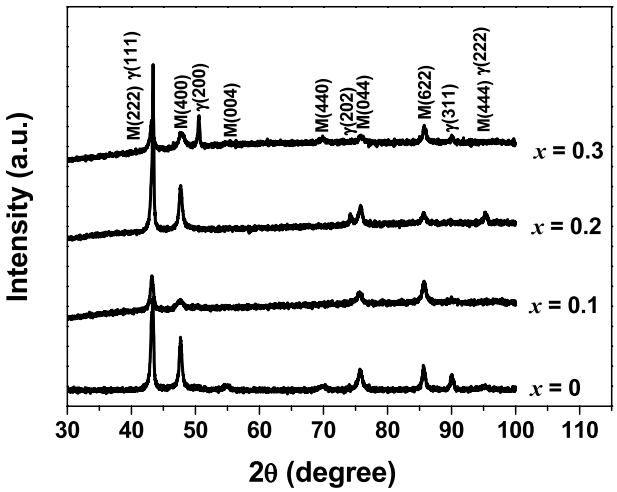

Figure 4. X-ray diffraction patterns of $(Ni_{53}Mn_{22}Co_6Ga_{19})_{100-x}Dy_x$ ($x = 0, 0.1, 0.2, 0.3$) alloys at room temperature.

increasing the Dy content, the c/a value and unit-cell volume show no obvious changes. The reasons are that the solubility of Dy in martensite is very low and the variation ($x = 0.1$–0.3) of Dy in this study is relatively small. The lattice parameters of the γ phase remain almost constant, being $a = 0.3613$ nm. No characteristic diffraction peaks of the Dy(Ni, Mn)$_4$Ga phase can be found in the x-ray patterns. This is probably due to the extremely low volume fraction of this compound. Previous studies have also indicated that diffraction peaks of Dy(Ni, Mn)$_4$Ga, Gd(Ni, Mn)$_4$Ga or Y(Ni, Mn)$_4$Ga are only observed when the Dy, Gd or Y contents in the alloys exceed 0.5 at.% [14–16, 18, 19].

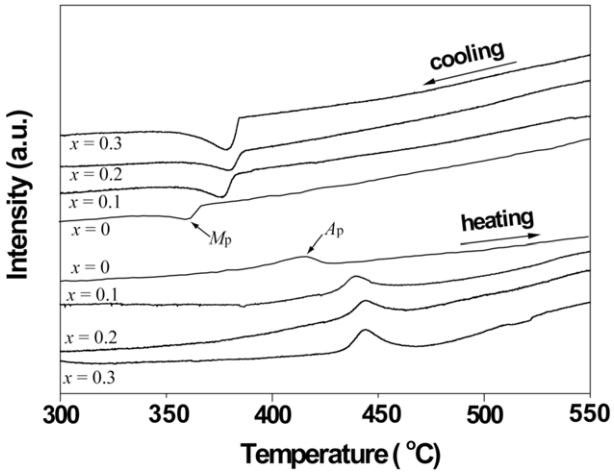

Figure 5. DSC curves of $(Ni_{53}Mn_{22}Co_6Ga_{19})_{100-x}Dy_x (x = 0, 0.1, 0.2, 0.3)$ alloys.

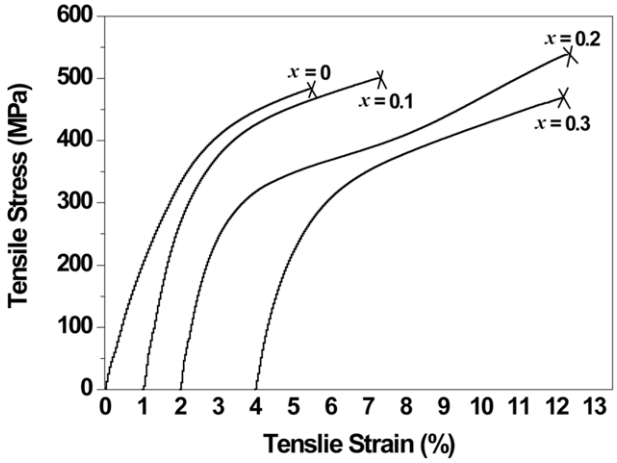

Figure 6. Tensile stress–strain curves of $(Ni_{53}Mn_{22}Co_6Ga_{19})_{100-x}Dy_x$ $(x = 0, 0.1, 0.2, 0.3)$ alloys at room temperature.

Table 2. The lattice parameters of martensite in $(Ni_{53}Mn_{22}Co_6Ga_{19})_{100-x}Dy_x$ $(x = 0, 0.1, 0.2, 0.3)$ alloys.

Samples	Lattice parameters (nm) a	c	c/a	Unit-cell volume (nm^3)
$x = 0$	0.7621	0.6581	0.864	0.3822
$x = 0.1$	0.7619	0.6695	0.879	0.3887
$x = 0.2$	0.7622	0.6660	0.874	0.3869
$x = 0.3$	0.7612	0.6667	0.876	0.3864

3.2. Martensitic transformation

Figure 5 shows the DSC curves of $(Ni_{53}Mn_{22}Co_6Ga_{19})_{100-x}Dy_x$ $(x = 0, 0.1, 0.2, 0.3)$ alloys. The martensitic transformations are reversible. The austenite and martensite transformation temperatures of the alloys are determined and listed in table 3. A_s, A_p, A_f are the starting, peak and finishing temperatures for austenite transformation, and M_s, M_p, M_f are the starting, peak and finishing temperatures for martensitic transformation, respectively. The hysteresis temperatures are equal to the difference between A_p and M_p. It can be seen that the reversible martensitic transformation temperatures abruptly increase (as high as 17 °C for M_p) at $x = 0.1$. But on further increasing the Dy content to 0.3 at.%, they only increase slightly (by 5.7 °C for M_p). Similar observations are observed in the previous investigations [18, 19].

In the present study, the changes of the martensitic transformation temperatures may be related to the combined effects of the changes in the tetragonality (c/a) and electron concentration (e/a) of martensite [1–3, 9–11, 23, 25, 26]. At $x = 0.1$, the dissolution of Dy in martensite results in a significant distortion of the crystal lattice (c/a), thereby leading to an abrupt increase in martensitic transformation temperature although the e/a of martensite decreases at the same time (table 1). With further increasing Dy content, the c/a has no obvious change, due to the very low solubility of Dy in martensite and relatively small concentration variation of Dy in this study ($x = 0.1$–0.3 at.%). Thus the martensitic transformation temperatures only increase slightly and the e/a of martensite also increases only slightly (table 1).

3.3. Mechanical properties and shape memory effect

Figure 6 shows the tensile stress–strain curves when $x = 0$, 0.1, 0.2 and 0.3, respectively. Symbol × in the figure represents the fracture point. The stress–strain curves are similar to those of two-phase Ni–Mn–Co–Ga HTSMAs [8, 9]. The tensile stress and strain are measured to be 483 MPa and 5.5% ($x = 0$), 500 MPa and 6.3% ($x = 0.1$), 538 MPa and 10.3% ($x = 0.2$), 426 MPa and 8.2% ($x = 0.3$), respectively. It appears that the refinement of grain size has a beneficial effect on the tensile ductility and strength of the alloys. As a result, the tensile ductility and strength of the alloys reach maximum values of 10.3% and 538 MPa at $x = 0.2$, respectively. Previous investigations [13–15] have found that a large amount of $Gd(Ni, Mn)_4Ga$ and $Y(Ni, Mn)_4Ga$ phases can improve the compressive ductility and strength of the single phase martensitic $Ni_{50}Mn_{29}Ga_{21}$ alloy. However, these results are apparently different from these of two-phase Ni–Mn–Co–Ga alloys with a small Dy

Table 3. Martensitic transformation temperatures of $(Ni_{53}Mn_{22}Co_6Ga_{19})_{100-x}Dy_x$ $(x = 0, 0.1, 0.2, 0.3)$ alloys.

Samples	A_s (°C)	A_p (°C)	A_f (°C)	M_s (°C)	M_p (°C)	M_f (°C)	Hysteresis (°C)
$x = 0$	397.4	413.7	428.6	365.8	359.6	346.9	54.1
$x = 0.1$	430.0	439.6	456.3	382.4	376.6	363.0	63.0
$x = 0.2$	434.1	443.6	458.5	385.7	380.2	365.6	63.4
$x = 0.3$	435.6	446.1	462.5	386.8	382.3	362.5	63.8

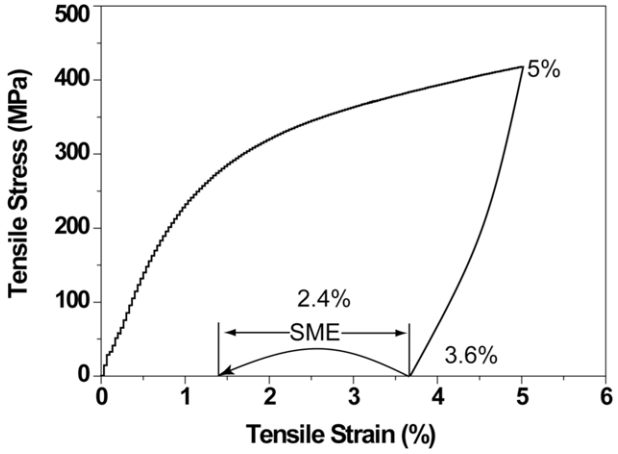

Figure 7. SME of $x = 0.3$ at a pre-strain of 5.0% according to the residual strain of 3.6%. The arrowed range represents the recovery strain after the sample was heated to 600 °C for 5 min.

addition in the present study. It is confirmed that the γ phase plays a major role on the ductility improvement in two-phase Ni–Mn–Co–Ga alloys [9]. However, the amount of $Dy(Ni, Mn)_4Ga$ precipitates in the $x = 0.3$ alloy may negatively affect the benefits of the γ phase on the ductility improvement, leading to a decrease in the tensile ductility and strength of the alloy at $x = 0.3$.

In order to investigate the SMEs of $(Ni_{53}Mn_{22}Co_6Ga_{19})_{100-x}Dy_x$ alloys, the plate samples were pre-strained to different degrees, and similar residual strains of about 3.6% and 4.8% were obtained. Figure 7 shows the stress–strain curve for $x = 0.3$ at a pre-strain of 5.0%. The corresponding residual strain is 3.6% after unloading. The range (arrowed) in the inset represents the recovery strain after the sample was heated to 600 °C for 5 min. The recoverable strain is 2.4%, corresponding to a recovery rate of 67%. Figure 8 shows the recovery strains (ε_{SME}) and recovery rates (R) under different residual strains of about 3.6% and 4.8% for $x = 0, 0.1, 0.2$ and 0.3. From figure 8, it can be found that when adding 0.1 at.% of Dy, the SMEs and recovery rates decrease, whereas they gradually increase on further increasing the Dy content. The reasons can be understood by considering the refinement of grain size. On the one hand, more grain boundaries form with the refinement of grain size following the Dy addition, which enhances the negative effect of the γ phase in hampering the martensite reorientation [6–10, 25]. This will lead to a decrease of SMEs and recovery rates. On the other hand, it has been reported that the martensite reorientation will proceed at a higher stress level with an increase in the critical stress for martensite reorientation in Ni–Mn–Ga HTSMAs [25]. Thus, it might cause the activation of dislocation gliding, which applies an opposite influence on the SME of Ni–Mn–Ga alloys. Therefore, it can be deduced that decreasing the critical stress for martensite reorientation may be an effective method to improve the SME of the present alloys. From figure 8, it can be seen that the yield strength obviously decreases on further increasing the Dy addition to 0.2 and 0.3 at.%. It implies that the martensite reorientation occurs more easily in the $x = 0.2$ and 0.3 alloys, thus giving rise to better SMEs than that of the $x = 0.1$ alloy.

4. Conclusions

In this study, the microstructures, martensitic transformation behaviors, mechanical and high-temperature shape memory properties of $(Ni_{53}Mn_{22}Co_6Ga_{19})_{100-x}Dy_x$ ($x = 0, 0.1, 0.2, 0.3$) alloys were investigated. The following conclusions can be drawn:

(1) A small Dy addition can refine the grain size, which can effectively improve the tensile ductility and strength of the two-phase $Ni_{53}Mn_{22}Co_6Ga_{19}$ alloy, up to maximum values of 10.3% and 538 MPa at $x = 0.2$, respectively. However, the tensile ductility and strength decrease on further increasing the Dy addition to 0.3 at.% due to the formation of a large number of $Dy(Ni, Mn)_4Ga$ precipitates.

(2) The change in the martensitic transformation temperatures of $(Ni_{53}Mn_{22}Co_6Ga_{19})_{100-x}Dy_x$ ($x = 0, 0.1, 0.2, 0.3$) alloys could be attributed to the combined effects of the changes in the c/a and e/a of martensite.

(3) The results further show that on adding 0.1 at.% of Dy, the SMEs and recovery rates of the alloys decrease due to the

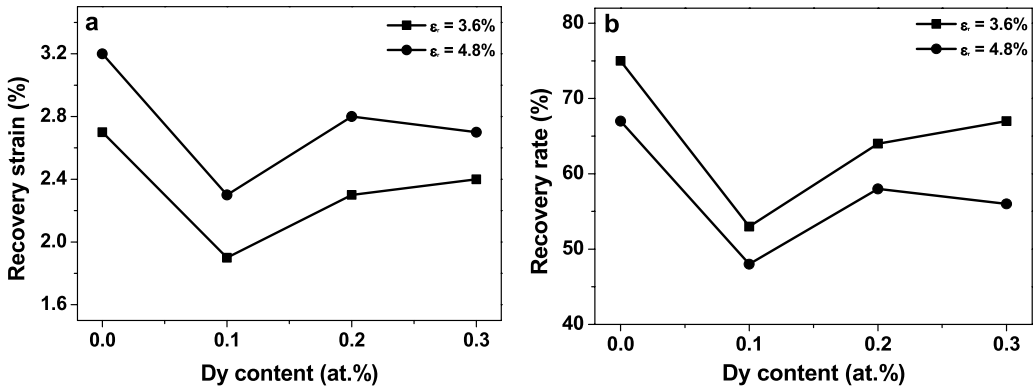

Figure 8. (a) Relationship between Dy content and recovery strains (ε_{SME}) under different residual strains (ε_r) of 3.6% and 4.8%. (b) Relationship between Dy content and recovery rates (R) under different residual strains (ε_r) of 3.6% and 4.8%.

refinement of grain size compared to those of the two-phase $Ni_{53}Mn_{22}Co_6Ga_{19}$ alloy, whereas they gradually increase on further increasing the Dy content to 0.2 and 0.3 at.% due to a decrease of the alloy strength.

Acknowledgments

This work was supported by the National Natural Science Foundation of China (Grant Nos. 51031003 and 51201145) and the Ministry of Science and Technology of China (Grant No. 2009DFA52170).

References

[1] Chernenko V A, Cesari E, Kokorin V V and Vitenko I N 1995 The development of new ferromagnetic shape memory alloys in Ni–Mn–Ga system *Scr. Metall. Mater.* **33** 1239–44

[2] Jin X, Marioni M, Bono D, Allen S M, O'Handley R C and Hsu T Y 2002 Empirical mapping of Ni–Mn–Ga properties with composition and valence electron concentration *J. Appl. Phys.* **91** 8222–5

[3] Jiang C B, Feng G, Gong S K and Xu H B 2003 Effect of Ni excess on phase transformation temperatures of NiMnGa alloys *Mater. Sci. Eng.* A **342** 231–5

[4] Xu H B, Ma Y Q and Jiang C B 2003 A high-temperature shape-memory alloy $Ni_{54}Mn_{25}Ga_{21}$ *Appl. Phys. Lett.* **82** 3206–8

[5] Ma Y Q, Jiang C B, Feng G and Xu H B 2003 Thermal stability of the $Ni_{54}Mn_{25}Ga_{21}$ Heusler alloy with high temperature transformation *Scr. Mater.* **48** 365–9

[6] Ma Y Q, Xu L H, Li Y, Jiang C B, Xu H B and Lee Y K 2005 Martensitic transformation, ductility, and shape-memory effect of polycrystalline $Ni_{56}Mn_{25-x}Fe_xGa_{19}$ alloys *Z. Metallk.* **96** 843–6

[7] Xin Y, Li Y, Chai L and Xu H B 2007 Shape memory characteristics of dual-phase Ni–Mn–Ga based high temperature shape memory alloys *Scr. Mater.* **57** 599–601

[8] Ma Y Q, Yang S Y, Wang C P and Liu X J 2008 Tensile characteristics and shape memory effect of $Ni_{56}Mn_{21}Co_4Ga_{19}$ high temperature shape memory alloy *Scr. Mater.* **58** 918–21

[9] Ma Y Q, Yang S Y, Liu Y and Liu X J 2009 The ductility and shape memory properties of Ni–Mn–Co–Ga high-temperature shape-memory alloys *Acta Mater.* **57** 3232–41

[10] Ma Y Q, Yang S Y, Jin W J and Liu X J 2009 $Ni_{56}Mn_{25-x}Cu_xGa_{19}$ ($x = 0, 1, 2, 4, 8$) high-temperature shape-memory alloys *J. Alloys Compounds* **471** 570–4

[11] Yang S Y, Liu Y, Wang C P and Liu X J 2012 Martensite stabilization and thermal cycling stability of two-phase NiMnGa-based high-temperature shape memory alloys *Acta Mater.* **60** 4255–67

[12] Tsuchiya K, Tsutsumi A, Ohtsuka H and Umemoto M 2004 Modification of Ni–Mn–Ga ferromagnetic shape memory alloy by addition of rare earth elements *Mater. Sci. Eng.* A **378** 370–6

[13] Cai W, Gao L, Liu A L, Sui J H and Gao Z Y 2007 Martensitic transformation and mechanical properties of Ni–Mn–Ga–Y ferromagnetic shape memory alloys *Scr. Mater.* **57** 659–62

[14] Sui J H, Zhang X, Gao L and Cai W 2011 Microstructure, phase transformation and mechanical properties of Ni–Mn–Ga–Y magnetic shape memory alloys *J. Alloys Compounds* **509** 8692–9

[15] Gao L, Cai W, Liu A L and Zhao L C 2006 Martensitic transformation and mechanical properties of polycrystalline $Ni_{50}Mn_{29}Ga_{21-x}Gd_x$ ferromagnetic shape memory alloys *J. Alloys Compounds* **425** 314–7

[16] Cai W, Gao L and Gao Z Y 2007 Microstructure and phase transformations in a $Ni_{50}Mn_{29}Ga_{16}Gd_5$ alloy with a high transformation temperature *J. Mater. Sci.* **42** 9216–20

[17] Gao L, Sui J H and Cai W 2008 Influence of rare earth Gd addition on the structural and magnetic transtions of Ni–Mn–Ga alloys *J. Magn. Magn. Mater.* **320** 63–7

[18] Gao L, Gao Z Y, Cai W and Zhao L C 2006 Effect of rare earth Dy addition on microstructure and martensitic transformation of polycrystalline $Ni_{50}Mn_{29}Ga_{21-x}Dy_x$ ferromagnetic shape memory alloys *Mater. Sci. Eng.* A **438** 1077–80

[19] Gao L, Sui J H, Cai W and Gao Z Y 2009 Study of the precipitate phases and martensitic transformation in quaternary Heusler alloys of NiMnGaDy *Solid State Commun.* **149** 257–60

[20] Dieter G E 1986 *Mechanical Metallurgy* (New York: McGraw-Hill) p 295

[21] Lee S Y and Nash P 1991 *Phase Diagrams of Binary Nickel Alloys* ed P Nash (Materials Park, OH: ASM International)

[22] Gokcen N A 1991 *Phase Diagrams of Binary Nickel Alloys* ed P Nash (Materials Park, OH: ASM International)

[23] Yang S Y, Wang C P and Liu X J 2012 Phase equilibria and composition dependence of martensitic transformation in Ni–Mn–Ga ternary system *Intermetallics* **25** 101–8

[24] Joshi D A, Tomy C V, Rana D S, Nagajan R and Malik S K 2006 Magnetic properties of ternary gallides of type RNi$_4$Ga (R = rare earths) *Solid State Commun.* **137** 225–9

[25] Ma Y Q, Jiang C B, Li Y, Xu H B, Wang C P and Liu X J 2007 Study of $Ni_{50+x}Mn_{25}Ga_{25-x}$ ($x = 2$–11) as high-temperature shape-memory alloys *Acta Mater.* **55** 1533–41

[26] Lanska N, Sōderberg O, Sozinov A, Ge Y, Ullakko K and Lindroos V K 2004 Composition and temperature dependence of the crystal structure of Ni–Mn–Ga alloys *J. Appl. Phys.* **95** 8074–8